Journal of Materials Chemistry

Cite this: J. Mater. Chem., 2011, 21, 15171

www.rsc.org/materials

COMMUNICATION

# Efficient synthesis of polymeric g-$C_3N_4$ layered materials as novel efficient visible light driven photocatalysts†

Fan Dong,*[a] Liwen Wu,[a] Yanjuan Sun,[a] Min Fu,[a] Zhongbiao Wu*[b] and S. C. Lee[c]

*Received 20th June 2011, Accepted 3rd August 2011*
**DOI: 10.1039/c1jm12844b**



**In order to develop efficient visible light driven photocatalysts for environmental applications, novel polymeric g-$C_3N_4$ layered materials with high surface areas are synthesized efficiently from an oxygen-containing precursor by directly treating urea in air between 450 and 600 °C, without the assistance of a template for the first time. The as-prepared g-$C_3N_4$ materials with strong visible light absorption have a band gap around 2.7 eV. The crystallinity and specific surface areas of g-$C_3N_4$ increases simultaneously when the heating temperatures increases. The g-$C_3N_4$ materials are demonstrated to exhibit much higher visible light photocatalytic activity than that of C-doped $TiO_2$ and g-$C_3N_4$ prepared from dicyanamide for the degradation of aqueous RhB. The large surface areas, layered structure and band structure in all contributed to the efficient visible light photocatalytic activity. The efficient synthesis method for g-$C_3N_4$ combined with efficient photocatalytic activity is of significant interest for environmental pollutants degradation and solar energy conversion in large scale applications.**

## 1. Introduction

The hunt for efficient semiconductor photocatalysts for pollutants degradation and splitting of water into hydrogen using solar energy (visible light) has been an intensifying endeavor worldwide.[1–5] During the past few decades, various types of photocatalytic materials that can work under visible light have been developed, such as non-metal doped $TiO_2$, composite metal oxides, metal sulfide and oxynitride, and noble metal based plasmonic photocatalysts.[6–15] Potential photocatalytic materials require a strong visible light response and high photocatalytic performance as well as the chemical stability.

Recently, Wang *et al.* reported the first novel stable metal-free photocatalyst, polymeric graphite-like carbon nitride (g-$C_3N_4$), which exhibits high photocatalytic performance for hydrogen generation from water splitting and degradation of organic dyes under visible light irradiation, and can be synthesized facilely by heating cyanamide.[16] The as-prepared g-$C_3N_4$ materials have low specific surface areas ($S_{BET}$) of ~10 $m^2$ $g^{-1}$ and the cyanamide as precursor is toxic. Although templates can be added in the synthesis process to increase the specific surface areas of g-$C_3N_4$, the synthesis procedure would become relatively tedious.[17–19] In general, the commonly used precursors for synthesis of g-$C_3N_4$ are reactive nitrogen-rich and oxygen-free compounds containing pre-bonded C–N core structures, such as cyanamide, dicyanamide, triazine and heptazine derivatives.[20–23] Many of the precursor compounds are difficult to obtain and expensive, and some of them are unstable, and/or even highly explosive. Very recently, mesoporous $TiO_2$ spheres prepared by a light-driven strategy were used for the activation of urea followed by HF etching to produce a g-$C_3N_4$ material.[24] The precursor urea, a nitrogen-rich, oxygen-containing compound, is cheap and easily available. However, such a process to prepare g-$C_3N_4$ with the assistance of $TiO_2$ is rather complicated and use of HF is not environmentally benign.

The present study reports the first transformation of urea into polymeric g-$C_3N_4$ with high specific surface areas by directly heating urea between 450 and 600 °C in air without the assistance of $TiO_2$ or other templates. Differing from previous oxygen-free precursors, the present urea contains oxygen, which may imply a new possible formation mechanism from urea to g-$C_3N_4$. The as-prepared g-$C_3N_4$ materials show enhanced visible light photocatalytic activity for degradation of aqueous Rhodamine (RhB), higher than that of C-doped $TiO_2$ and g-$C_3N_4$ prepared from dicyanamide. To the best of our knowledge, our method is probably the simplest and most economic approach to prepare efficient visible light driven photocatalysts. Therefore, the efficient synthesis approach is highly attractive and ready for large scale environmental and energetic applications.

## 2. Experimental

### 2.1. Synthesis of g-$C_3N_4$

The polymeric g-$C_3N_4$ was prepared by a facile and efficient method. In a typical synthesis, 10 g of urea powder was put into an alumina crucible with a cover, and then heated to a certain temperature in the range of 450 and 600 °C in a muffle furnace for 2 h at a heating rate of 15 °C $min^{-1}$. The resultant yellow powder was collected for use

[a]*College of Environmental and Biological Engineering, Chongqing Technology and Business University, Chongqing, 400067, P. R. China. E-mail: dfctbu@126.com*
[b]*Department of Environmental Engineering, Zhejiang University, Hangzhou, 310027, P. R. China. E-mail: zbwu@zju.edu.cn*
[c]*Department of Civil and Structural Engineering, Research Center for Environmental Technology and Management, The Hong Kong Polytechnic University, Hong Kong, P. R. China*
† Electronic supplementary information (ESI) available: Fig. S1–S5. See DOI: 10.1039/c1jm12844b

without further treatment. For comparison, C-doped $TiO_2$ (C–$TiO_2$) was prepared by a hydrothermal method.[25] g-$C_3N_4$ was also synthesized from dicyanamide according to the literature (CN-R).[22] These two samples were used as references.

### 2.2. Characterization

The crystal phases of the sample were analyzed by X-ray diffraction with Cu Kα radiation (XRD: model D/max RA, Rigaku Co., Japan). FT-IR spectra were recorded on a Nicolet Nexus spectrometer on samples embedded in KBr pellets. X-Ray photoelectron spectroscopy with Al Kα X-rays ($h\nu$ =1486.6 eV) radiation operated at 150 W (XPS: Thermo ESCALAB 250, USA) was used to investigate the surface properties. The shift of the binding energy due to relative surface charging was corrected using the C1s level at 284.8 eV as an internal standard. A scanning electron microscope (SEM, JEOL model JSM-6490, Japan) was used to characterize the morphology of the obtained products. The morphology and structure of the samples were examined by transmission electron microscopy (TEM: JEM-2010, Japan). The UV-vis diffuse reflection spectra were obtained for the dry-pressed disk samples using a Scan UV-vis spectrophotometer (UV-vis DRS: UV-2450, Shimadzu, Japan) equipped with an integrating sphere assembly, using $BaSO_4$ as reflectance sample. The spectra were recorded at room temperature in air that ranged from 250 to 800 nm. The photoluminescence spectra were measured with a fluorescence spectrophotometer (PL: FS-2500, Japan) using a Xe lamp as an excitation source with optical filters. Nitrogen adsorption–desorption was conducted on a nitrogen adsorption apparatus (ASAP 2020, USA). All the samples were degassed at 150 °C prior to measurements.

### 2.3. Evaluation of visible light photocatalytic activity

Photocatalytic activity of g-$C_3N_4$ for RhB photodegradation was evaluated in a quartz glass reactor. 0.05 g of g-$C_3N_4$ was dispersed in RhB aqueous solution (55 mL, 5 mg $L^{-1}$). The light irradiation system contains a 500 W Xe lamp with a jacket filled with flowing and thermostatted aqueous $NaNO_2$ solution (1 M) between the lamp and the reaction chamber as a filter to block UV light ($\lambda < 400$ nm) and eliminate the temperature effect. The suspension was first allowed to reach adsorption–desorption equilibrium with continuous stirring for 60 min in the dark prior to irradiation. The degradation rate of RhB was evaluated using the UV-vis absorption spectra to measure the peak value of a maximum absorption of RhB solution. During the irradiation, 5 mL of suspension was continually taken from the reaction cell at given time intervals for subsequent dye concentration analysis after centrifugation. The RhB solution shows a similar pH value at 6.8, which does not affect the light absorption of RhB. The maximum absorption of RhB is at wavelength of 552 nm. The degradation rate $\eta$ (%) can be calculated as:

$$\eta\ (\%) = (C_0 - C)/C_0 \times 100\%$$

Where, $C_0$ is the initial concentration of RhB considering RhB adsorption on the catalyst and $C$ is the revised concentration after irradiation.

## 3. Result and discussion

XRD (Fig. 1a) reveals the graphite like packing for all $C_3N_4$ materials obtained under different temperatures between 450 and 600 °C. The typical (002) interlayer-stacking peak around 27.6° corresponds to an interlayer distance of $d = 0.33$ nm for CN-550, as is well-known for g-$C_3N_4$. Further observation indicates that the (002) peak shifts toward higher diffraction angles from CN-450 of 27.2° to CN-600 of 27.7° with increased treatment temperatures (Fig. S1†). This fact suggests that the crystal structure of g-$C_3N_4$ tends to become more stable under high temperature. The peak at 13.0° corresponding to in-plane ordering of tri-*s*-triazine units, which form 1D melon strands also increased with increasing temperatures. When the treating temperature is lower than 400 °C, g-$C_3N_4$ cannot be produced.

Fig. 1b shows the FT-IR spectra of the materials prepared under different temperatures. The bands of CN-400 agree with those in the spectra of cyanuric acid. This implies that the urea condensed to form a cyanuric acid like compound first at 400 °C. When the temperature is higher than 450 °C, g-$C_3N_4$ can be produced. As can be seen from Fig. 1b, several bands in the 1200–1650 $cm^{-1}$ region corresponding to the typical stretching modes of CN heterocycles are found for g-$C_3N_4$ prepared above 450 °C. The characteristic mode of the triazine units at 801 $cm^{-1}$ is also observed.[26] The broad bands at around 3300 $cm^{-1}$ are indicative of stretching vibration modes for –NH (Fig. S2†).[26] The formation mechanism of g-$C_3N_4$ from urea during thermal treatment is in progress.

The C1s spectrum in Fig. S3a† shows that two main carbon species with binding energies of 286.5 and 288.3 eV, corresponding to C–N–C and C–$(N)_3$, are present in the CN-575.[24] Three binding

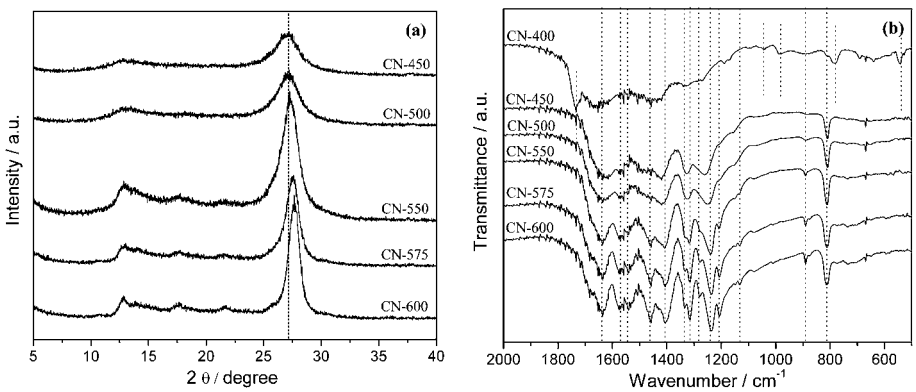


**Fig. 1** XRD patterns (a) and FT-IR spectra in the range of 500–2000 $cm^{-1}$ (b) of materials obtained under different temperatures.

 

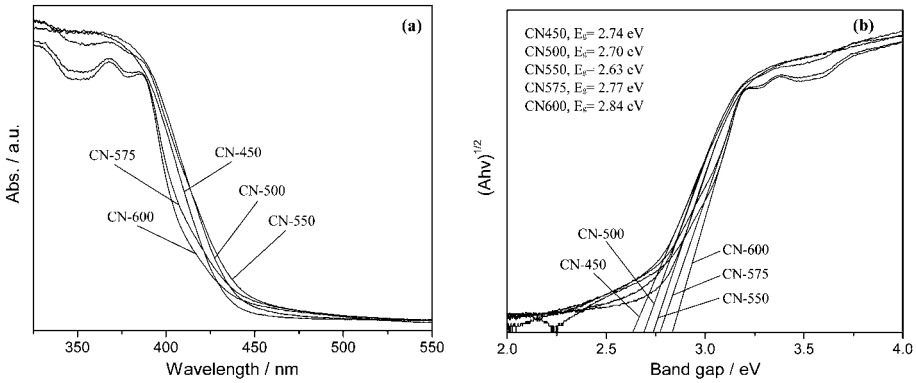


**Fig. 2** UV-vis DRS (a) and plots of $(Ahv)^{1/2}$ *vs.* photon energy (b) of g-$C_3N_4$ obtained under different temperatures.

energies in N1s region (Fig. S3b†) can be observed, which can be ascribed to C–N–C (398.8 eV), N–$(C)_3$ (400.1 eV) and N–H groups (401.2 eV), respectively.[24] The O1s peak at 533.0 eV is assignable to the adsorbed $H_2O$ on the materials surface.[27]

The UV-vis DRS of g-$C_3N_4$ obtained under different temperatures are shown in Fig. 2a. It can be seen that all the samples exhibit strong visible light absorption with absorption edges at around 450 nm. When the temperature increases, the absorption edge first shifts up until the temperature reaches 550 °C, then the absorption edge decreases. The band gap energy ($E_g$) can be estimated from the intercept of the tangents to the plots of $(Ahv)^{1/2}$ *vs.* photon energy, as shown in Fig. 2b.[27] The calculated $E_g$ value is around 2.7 eV, consistent with previous reports.[16,26]

For g-$C_3N_4$ prepared at 450 °C, the agaric like layers are smooth and flat (Fig. 3a). A large number of layers with a thickness of about 30 nm are packed together. The TEM image (Fig. 3b) indicates that the ordered non-crystalline structure goes nicely with the XRD data. For the CN-575 sample, like tremella, the area of single layer becomes large and the thickness is reduced to about 20 nm (Fig. 3c). Further observation on a SEM picture indicates that there are some pores on the layers' surface. The TEM image (Fig. 3d) shows the layers are buckled and backfolded at their edges.

Fig. S4† shows the room temperature PL spectra for CN-450 and CN-575 samples using the excitation light of 280 nm. It can also be seen that the PL intensity of CN-450 is much higher than that in the spectra of CN-575, indicating that recombination of photogenerated electrons and holes can be effectively inhibited on CN-575. The enhanced crystallinity due to higher temperature treatment (see Fig. 1a) facilitates the separation of charge carriers, thus contributing to the lower PL intensity.

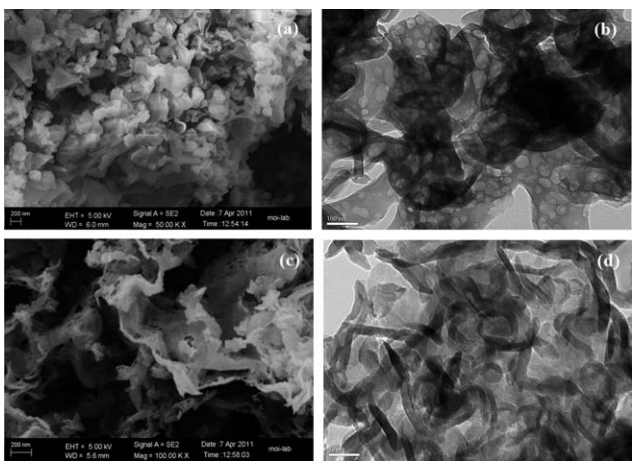


**Fig. 3** SEM (a) and (b) TEM images of CN-450, SEM (c) and (d) TEM images of CN-575.

Fig. 4a shows the correlation between the $S_{BET}$ of g-$C_3N_4$ and the thermal treating temperatures. Generally speaking, the $S_{BET}$ decreases with increasing temperatures as the crystallinity is enhanced gradually due to high temperature treatment (see Fig. 1a). However, it is very interesting to note that the $S_{BET}$ of g-$C_3N_4$ increases from 12.23 to 96.6 $m^2\ g^{-1}$ when the treating temperature increases from 450 to 600 °C. This fact implies that the formation mechanism of g-$C_3N_4$ from urea is different from traditional materials, although, the formation mechanism is currently not clear. The $S_{BET}$ of as-synthesized CN-600 is much higher than that of g-$C_3N_4$ prepared from cyanamide (10.0 $m^2\ g^{-1}$).[16]

Fig. 4b shows the adsorption property and photocatalytic activities of the g-$C_3N_4$ obtained under different temperatures for degradation of RhB under visible light. It can be seen that the adsorption–desorption equilibrium has been reached within 60 min. The amounts of RhB adsorbed by different g-$C_3N_4$ samples increase when the treatment temperature increases, consistent with the value of the specific surface areas for the samples. The photodegradation of RhB over C-doped $TiO_2$ and the g-$C_3N_4$ obtained by heating dicyanamide at 550 °C for 2 h (CN-R) was also given here for comparison. When there is no photocatalyst involved with visible light irradiation, the organic contaminant RhB is stable, which indicates that self-degradation was negligible. The RhB undergoes pronounced decomposition in the presence of various photocatalysts under visible light irradiation. Although the C-doped $TiO_2$ has a high specific surface area of 122.5 $m^2\ g^{-1}$, higher than that of all g-$C_3N_4$ samples, it is obvious that photocatalytic activities for all the g-$C_3N_4$ samples are much higher than that of the C–$TiO_2$, which implies that g-$C_3N_4$ is an excellent photocatalyst for degradation of organic dyes. The special layered 2D structure and band structure may contribute to the excellent visible light photocatalytic performance. Further observation indicates that the g-$C_3N_4$ samples prepared from urea exhibit much more efficient photocatalytic activity than that of CN-R prepared from dicyanamide. For g-$C_3N_4$ prepared at the same temperature from different precursors, CN-550 (64.3 $m^2\ g^{-1}$) reaches a maximum removal rate of 100% (see Fig. S5†), five times higher than that of CN-R sample (8.0 $m^2\ g^{-1}$) with a removal rate of 19%.

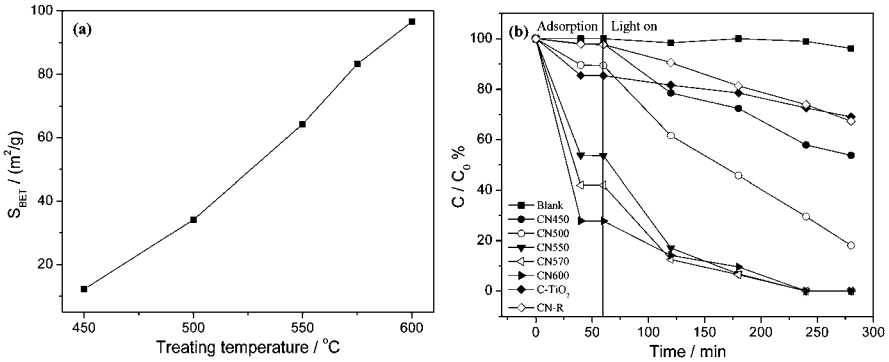


**Fig. 4** The correlation between $S_{BET}$ and thermal treatment temperatures (a) adsorption property and photocatalytic activities of the g-$C_3N_4$ obtained under different temperatures for degradation of RhB under visible light (b).

The high specific surface areas mainly contributed to the enhanced activity of CN-550, as large surface areas are favorable for the adsorption of reactants and diffusion of reaction products.[28,29] Considering the energy consumption and photocatalytic performance, heating temperature of 550 °C for 2 h is an optimized synthesis condition. For the first time, significant advances have been made on the efficient and facile synthesis of novel polymeric g-$C_3N_4$ layered materials with efficient visible light photocatalytic activity. As the precursor urea is cheap and easily available and the synthesis method is very facile, our efficient synthesis approach for g-$C_3N_4$ is extremely attractive and valuable, and therefore, ready for large scale environmental and energy applications.

## 4. Conclusion

Polymeric g-$C_3N_4$ layered materials with high surface areas (up to 96.6 $m^2$ $g^{-1}$) were successfully synthesized from an oxygen-containing precursor by directly heating urea in air between 450 and 600 °C for the first time. The g-$C_3N_4$ materials have a band gap around 2.7 eV, suitable for visible light utilization. As the heating temperature increases, the crystallinity and specific surface areas of g-$C_3N_4$ increases simultaneously. The as-prepared g-$C_3N_4$ exhibited much higher visible light photocatalytic activity than that of C-doped $TiO_2$ and g-$C_3N_4$ prepared from dicyanamide for the degradation of aqueous RhB. The large surface areas, layered structure and suitable band structure, in all, contributed to the efficient visible light photocatalytic activity. The efficient synthesis method for g-$C_3N_4$ combined with efficient visible light photocatalytic activity is of significant interest for pollutants degradation and solar energy conversion in large scale applications.

## Acknowledgements

This research is financially supported by National High Technology Research and Development Program (863 Program) of China (2010AA064905), Zhejiang Provincial Engineering Research Center of Industrial Boiler & Furnace Flue Gas Pollution Control (No. 2010B01), Research Grants of Chongqing Technology and Business University (2010-56-13, 113013), the Program for Chongqing Innovative Research Team Development in University (KJTD201020), and The Chongqing Key Natural Science Foundation (CSTC, 2008BA4012).

## References and notes

1 A. Kudo and Y. Miseki, *Chem. Soc. Rev.*, 2009, **38**, 253.
2 C. C. Chen, W. H. Ma and J. C. Zhao, *Chem. Soc. Rev.*, 2010, **39**, 4206.
3 G. Liu, L. Z. Wang, H. G. Yang, H. M. Cheng and G. Q. Lu, *J. Mater. Chem.*, 2010, **20**, 831.
4 D. Q. Zhang, G. S. Li and J. C. Yu, *J. Mater. Chem.*, 2010, **20**, 4529.
5 J. L. Zhang, Y. M. Wu, M. Y. Xing, S. A. K. Leghari and S. Sajjad, *Energy Environ. Sci.*, 2010, **3**, 715.
6 A. Fujishima, X. T. Zhang and D. A. Tryk, *Surf. Sci. Rep.*, 2008, **63**, 515.
7 L. S. Zhang, W. Z. Wang, L. Zhou and H. L. Xu, *Small*, 2007, **3**, 1618.
8 S. X. Ge and L. Z. Zhang, *Environ. Sci. Technol.*, 2011, **45**, 3027.
9 L. W. Zhang, T. G. Xu, X. Zhao and Y. F. Zhu, *Appl. Catal., B*, 2010, **98**, 138.
10 Y. N. Huo, M. Miao, Y. Zhang, J. Zhu and H. X. Li, *Chem. Commun.*, 2011, **47**, 2089.
11 X. Xiao and W. D. Zhang, *J. Mater. Chem.*, 2010, **20**, 5866.
12 J. J. Wu, F. Q. Huang, X. J. Lu, P. Chen, D. Y. Wan and F. F. Xu, *J. Mater. Chem.*, 2011, **21**, 3872.
13 K. Maeda and K. Domen, *Chem. Mater.*, 2010, **22**, 612.
14 F. Dong, H. Q. Wang, G. Sen, Z. B. Wu and S. C. Lee, *J. Hazard. Mater.*, 2011, **187**, 509.
15 F. Dong, H. Q. Wang, Z. B. Wu and J. F. Qiu, *J. Colloid Interface Sci.*, 2010, **343**, 200.
16 X. C. Wang, K. Maeda, A. Thomas, K. Takanabe, G. Xin, J. M. Carlsson, K. Domen and M. Antonietti, *Nat. Mater.*, 2009, **8**, 76.
17 X. Jin, V. V. Balasubramanian, S. T. Selvan, D. P. Sawant, M. A. Chari, G. Q. Lu and A. Vinu, *Angew. Chem., Int. Ed.*, 2009, **48**, 7884.
18 F. Z. Su, S. C. Mathew, G. Lipner, X. Z. Fu, M. Antonietti, S. Blechert and X. C. Wang, *J. Am. Chem. Soc.*, 2010, **132**, 16299.
19 K. Takanabe, K. Kamata, X. C. Wang, M. Antonietti, J. Kubota and K. Domen, *Phys. Chem. Chem. Phys.*, 2010, **12**, 13020.
20 B. Jurgens, E. Irran, J. Senker, P. Kroll, H. Mu ller and W. Schnick, *J. Am. Chem. Soc.*, 2003, **125**, 10288.
21 J. R. Holst and E. G. Gillan, *J. Am. Chem. Soc.*, 2008, **130**, 7373.
22 M. J. Bojdys, J. Mller, M. Antonietti and A. Thomas, *Chem.–Eur. J.*, 2008, **14**, 8177.
23 J. S. Zhang, X. F. Chen, K. Takanabe, K. Maeda, K. Domen, J. D. Epping, X. Z. Fu, M. Antonietti and X. C. Wang, *Angew. Chem., Int. Ed.*, 2010, **49**, 441.
24 X. X. Zou, G. D. Li, Y. N. Wang, J. Zhao, C. Yan, M. Y. Guo, L. Li and J. S. Chen, *Chem. Commun.*, 2011, **47**, 1066.
25 F. Dong, H. Q. Wang and Z. B. Wu, *J. Phys. Chem. C*, 2009, **113**, 16717.
26 S. C. Yan, Z. S. Li and Z. G. Zou, *Langmuir*, 2009, **25**, 10397.
27 F. Dong, S. Guo, H. Q. Wang, X. F. Li and Z. B. Wu, *J. Phys. Chem. C*, 2011, **115**, 13285.
28 J. G. Yu, Y. R. Su and B. Cheng, *Adv. Funct. Mater.*, 2007, **17**, 1984.
29 X. X. Yu, J. G. Yu, B. Cheng and M. Jaroniec, *J. Phys. Chem. C*, 2009, **113**, 17527.

 